DOI: 10.1093/jnci/djs210
Advance Access publication on April 24, 2012.

ARTICLE

Glycogen Synthase Kinase-3β, NF-κB Signaling, and Tumorigenesis of Human Osteosarcoma

Qing-Lian Tang*, Xian-Biao Xie*, Jin Wang*, Qiong Chen, An-Jia Han, Chang-Ye Zou, Jun-Qiang Yin, Da-Wei Liu, Yi Liang, Zhi-Qiang Zhao, Bi-Cheng Yong, Ru-Hua Zhang, Qi-Sheng Feng, Wu-Guo Deng, Xiao-Feng Zhu, Binhua P. Zhou, Yi-Xin Zeng, Jing-Nan Shen, Tiebang Kang

Manuscript received June 7, 2011; revised March 20, 2012; accepted March 21, 2012.

Correspondence to: Tiebang Kang, PhD, State Key Laboratory of Oncology in South China, Sun Yat-Sen University Cancer Center, Guangzhou 510060, China (e-mail: kangtb@mail.sysu.edu.cn) or Jing-Nan Shen, MD, PhD, Department of Musculoskeletal Oncology, First Affiliated Hospital, Sun Yat-Sen University, Guangzhou 510080, China (e-mail: shenjingnan@21cn.com).

*Authors contributed equally to this work.

Background Glycogen synthase kinase-3β (GSK-3β), a serine/threonine protein kinase, may function as a tumor suppressor or an oncogene, depending on the tumor type. We sought to determine the biological function of GSK-3β in osteosarcoma, a rare pediatric cancer for which the identification of new therapeutic targets is urgent.

Methods We used cell viability assays, colony formation assays, and apoptosis assays to analyze the effects of altered GSK-3β expression in U2OS, MG63, SAOS2, U2OS/MTX300, and ZOS osteosarcoma cell lines. Nude mice (n = 5–8 mice per group) were injected with U2OS/MTX300, and ZOS cells to assess the role of GSK-3β in osteosarcoma growth in vivo and to evaluate the effects of inhibitors and/or anticancer drugs on tumor growth. We used an antibody array, polymerase chain reaction, western blotting, and a luciferase reporter assay to establish the effect of GSK-3β inhibition on the nuclear factor-κB (NF-κB) pathway. Immunochemistry was performed on primary tumor specimens from osteosarcoma patients (n = 74) to determine the relationship of GSK-3β activity with overall survival.

Results Osteosarcoma cells with low levels of inactive p-Ser9-GSK-3β formed colonies in vitro and tumors in vivo more readily than cells with higher levels and cells in which GSK-3β had been silenced formed fewer colonies and smaller tumors than parental cells. Silencing or pharmacological inhibition of GSK-3β resulted in apoptosis of osteosarcoma cells. Inhibition of GSK-3β resulted in inhibition of the NF-κB pathway and reduction of NF-κB-mediated transcription. Combination treatments with GSK-3β inhibitors, NF-κB inhibitors, and chemotherapy drugs increased the effectiveness of chemotherapy drugs in vitro and in vivo. Patients whose osteosarcoma specimens had hyperactive GSK-3β, and nuclear NF-κB had a shorter median overall survival time (49.2 months) compared with patients whose tumors had inactive GSK-3β and NF-κB (109.2 months).

Conclusion GSK-3β activity may promote osteosarcoma tumor growth, and therapeutic targeting of the GSK-3β and/or NF-κB pathways may be an effective way to enhance the therapeutic activity of anticancer drugs against osteosarcoma.

J Natl Cancer Inst 2012;104:749–763

Osteosarcoma is the most common primary malignant bone tumor in childhood and adolescence (1) and has a propensity for local invasion and early lung metastasis. Currently, 5-year survival from osteosarcoma remains at approximately 65%–70% for localized disease but at only 20% for metastatic disease, with only modest therapeutic improvement over the past 15 years (2,3) because current therapies often result in chemoresistance. It is urgent to further understand the mechanism of tumorigenesis in osteosarcoma to identify new therapeutic targets (4).

Glycogen synthase kinase-3β (GSK-3β) is a serine/threonine protein kinase that plays key roles in multiple pathways, and its dysregulation is implicated in many disorders, such as neurodegenerative diseases and cancers (5,6). However, the function of GSK-3β in cancer can differ depending on cell type. One of the most well-known substrates of GSK-3β, β-catenin, is an important regulator of the Wnt–β-catenin signaling pathway. Phosphorylation of β-catenin by GSK-3β results in ubiquitin-mediated degradation of β-catenin, reducing translocation of β-catenin into the nucleus. Consequently, the transcription of many proto-oncogenes, such as c-myc and cyclin D1, is dramatically suppressed. Hence, classically, GSK-3β is recognized as a tumor suppressor that is frequently inactivated in a variety of tumors (7). However, emerging evidence has shown that GSK-3β may actually promote the development of several cancer types, such as mixed lineage leukemia (8–10), glioma (11), and oral cancer (7). Therefore, the biological function of GSK-3β requires assessment in each type of tumor.

CONTEXT AND CAVEATS

Prior knowledge

Glycogen synthase kinase-3β (GSK-3β), an important serine-threonine protein kinase, has been reported to act as a tumor suppressor or an oncogene in various tumors, but its role in osteosarcoma was unknown.

Study design

Osteosarcoma cell lines that expressed various levels of GSK-3β were compared in terms of their viability, apoptosis, ability to form colonies in vitro, and ability to form tumors in nude mice. Mice carrying U2OS/MTX300 and ZOS cell xenografts were used to test the therapeutic effects of GSK-3β inhibitors with or without other cancer drugs. An antibody array and other techniques were used to study the effects of GSK-3β inhibition. Immunohistochemistry on clinical ostesosarcoma specimens was used to examine whether GSK-3β activation was associated with overall survival.

Contribution

The ability of osteosarcoma cells to form colonies and tumors appeared to be directly related to their levels of GSK-3β activity. Inhibition of GSK-3β activity resulted in inhibition of the nuclear factor-κB (NF-κB) pathway and in apoptosis of osteosarcoma cells. Combinations with GSK-3β inhibitors and/or NF-κB inhibitors increased the effectiveness of chemotherapy drugs vs osteosarcoma tumors in mouse models. Patients with osteosarcomas that expressed more inactive GSK-3β and NF-κB lived longer than patients whose tumors appeared to express more active forms.

Implications

GSK-3β activity appears to promote the growth of osteosarcomas via the NF-κB pathway. Therapies that target these pathways may be useful in the treatment of osteosarcoma.

Limitations

GSK-3β activity was not directly measured, and the contribution of GSK-3α was not addressed. Therapeutic treatment of osteosarcoma cells in vitro or in mouse models may not be representative of the potential effects in human patients.

From the Editors

The nuclear factor-κB (NF-κB) transcription factor is activated by a variety of cellular and developmental signals (12–15). Deregulated activation of NF-κB has been causally linked to the development of several human pathologies, including cancers (12–15). In fact, hyperactivation of NF-κB signaling contributes to chemoresistance in tumors (16) and tumorigenicity (17), and the NF-κB pathway has been reported to be involved in proliferation and differentiation of osteosarcoma cells (18–20). However, the molecular mechanism of NF-κB in chemoresistance of osteosarcoma still remains poorly understood.

To better understand the function of GSK-3β in osteosarcoma, here, we sought to determine whether GSK-3β can activate the NF-κB pathway to promote tumorigenicity and whether targeting of the GSK-3β and/or NF-κB pathways might represent a promising strategy to enhance the therapeutic activity of anticancer drugs against osteosarcoma. We first performed cell viability and apoptosis assays to assess the association of GSK-3β with osteosarcoma cell survival and then used mouse models to investigate the role of GSK-3β in tumorigenicity in vivo. Finally, tissue samples were subjected to immunohistochemistry to evaluate whether GSK-3β activation is associated with clinical outcomes of patients with osteosarcoma.

Materials and Methods

Cell Lines

Three human osteosarcoma cell lines (U2OS, MG63, SAOS2) and one osteoblast cell line (hFOB1.19) were cultured according to the instructions from American Type Culture Collection (ATCC). U2OS/MTX300 cells, a methotrexate-resistant derivative of the U2OS human osteosarcoma cell line, and ZOS and ZOS-M, syngeneic human osteosarcoma cell lines derived from a primary tumor and metastasis, respectively, from the same patient, were described previously (8,21). All of the cell lines and the primary cell cultures were grown in Dulbecco's modified Eagle medium (Invitrogen, Grand Island, NY) supplemented with 10% fetal bovine serum (Invitrogen) at 37°C and 5% CO_2. U2OS, MG63, SAOS2, and U2OS/MTX300 cells were gifts from Dr M. Serra (Istituti Ortopedici Rizzoli, Bologna, Italy). The osteoblast cell line (hFOB1.19) was obtained from the Cell Bank of the Chinese Academy of Sciences (Shanghai, China).

Plasmids

Plasmids encoding the human IκBα mutant (IκBα-mut), in which two serine residues at both 32 and 36 were changed into alanine residues, and p65 were gifts from Dr Jiong Deng (Shanghai Jiaotong University, Shanghai, China) (22). V5-tagged kinase-inactive (KD) and constitutively active (CA) GSK-3β were previously described (23). The GSK-3β–short hairpin RNA (shRNA) plasmid was obtained from GenePharma (Shanghai, China).

Antibodies and Reagents

Antibodies against GSK-3β (rabbit monoclonal, 1:1000), phosphorylated-Ser9-GSK-3β (rabbit monoclonal, 1:1000), phosphorylated-Ser32-IκBα (rabbit monoclonal, 1:1000), xIAP (rabbit monoclonal, 1:1000), cIAP-1 (rabbit monoclonal, 1:1000), and survivin (mouse monoclonal, 1:1000) were obtained from Cell Signaling Technology (Danvers, MA). Antibodies against GSK-3α/β (mouse monoclonal, 1:500), caspase-3 (mouse monoclonal, 1:500), IκBα (rabbit monoclonal, 1:250), p65 (mouse monoclonal, 1:500), and bcl-2 (mouse monoclonal, 1:250) were from Santa Cruz Biotechnology (Santa Cruz, CA). Lithium chloride (LiCl, 1M stock in water), SB216763 (10 mM stock in DMSO), doxorubicin (also known as adriamycin, ADM), methotrexate (MTX), cisplatin (DDP), 3-(4, 5-dimethylthiazol-2-yl)-2, 5-diphenyltetrazolium bromide (MTT), and the NF-κB inhibitors, pyrrolidine dithiocarbamate (PDTC, 1 mM stock in water), parthenolide (PARTH, 200 μM stock in DMSO), and Bay 11-7085 (BAY, 250 μM stock in DMSO), were purchased from Sigma (St Louis, MO). The specificity of PDTC, PARTH, and BAY for NF-κB was tested and confirmed previously (24–29).

Transient and Stable Transfections

Small interfering RNA (siRNA) against GSK-3β (sense, 5′-CUCAA GAACUGUCAAGUAAdTdT-3′; antisense, 5′-UUACUUGACA GUUCUUGAGdTdT-3'), IκBα (sense, 5′-CUCCGAGACUUUCG

AGGAAdTdT-3'; antisense, 5'-UUCCUCGAAAGUCUCGGAG dTdT-3'), and p65 (sense, 5'-CCAUCAACUAUGAUGAGUU dTdT-3';antisense 5'-AACUCAUCAUAGUUGAUGGTdGd-3') were synthesized by RiboBio (Guangzhou, China). Procedures for transient and stable transfection were as previously described (30,31). Briefly, targeting siRNAs at a final concentration of 100 nM were transfected into U2OS cells at 30%–50% confluence in six-well plates using Lipofectamine 2000 (Invitrogen). Cells were harvested with trypsin 72 hours after transfection with siRNA.

Colony Formation and Tumorigenicity Assays

Colony formation assays were performed as described (31). Briefly, osteosarcoma cells were plated in triplicate at 100 cells per well in six-well plates. After culture in Dulbecco's modified Eagle medium supplemented with 10% fetal bovine serum for 14 days, cell clones were washed three times with phosphate-buffered saline (PBS), fixed in methanol for 10 minutes, and dyed with crystal violet for 10 minutes at room temperature. Afterward, the dye was washed off and colonies that contained more than 50 cells were counted.

For tumorigenicity assays, osteosarcoma cell lines U2OS, SAOS2, MG63, ZOS, ZOS-M, or U2OS/MTX300, or U2OS cells that were stably transfected with empty vector, KD GSK-3β, or CA GSK-3β were injected near the axillary fossa subcutaneously (1×10^6 cells in 200 μL of PBS per Balb/c nude mouse, 6- to 8-weeks old, female; five mice per group), and the mice were monitored for 8 weeks. For stable cell lines in which GSK-3β expression was reduced using siRNA, the tumor size was measured with a sliding caliper every 3 days for 25 days, and the tumor volume was calculated using the formula $V = 1/2$ (width^2 × length). When length of the tumor was more than 1.5 cm, the experiment was stopped and the mice were killed by cervical dislocation, according to the protocol developed by the Guidance of Institutional Animal Care and Use Committee at Sun Yat-Sen University.

Cell Viability Assay

Osteosarcoma cell lines U2OS, U2OS/MTX300, SAOS2, MG63, ZOS, and ZOS-M were seeded in 96-well plates at a density of 3000 cells per well. They were treated with different concentrations of LiCl (1–20 mM), SB216763 (1–40 μM), inhibitor IX (0.5–8 μM), chemotherapy drugs (ADM, 4 ng/mL; MTX, 5 ng/mL; DDP, 200 ng/mL), and/or NF-kB inhibitors (PDTC, 10 μM; PARTH, 2 μM; BAY, 2.5 μM) for the indicated number of hours, and cell viability was measured by MTT assay as described (21).

Caspase-3 Activity Assay

To assess the cell viability of osteosarcoma cells after the indicated treatments, caspase-3 activity assays were performed according to the manufacturer's instructions (Calbiochem, Billerica, MA). Briefly, after cellular protein was extracted from treated osteosarcoma cells, protein concentrations were determined using the Bradford protein assay. Then, 10 μL of caspase-3 substrate was added to 30 μg of extracted cellular protein, and after incubation for 2 hours, caspase-3 activity was measured at 405 nm with a microtiter plate reader as recommended in the manufacturer's instructions.

Dual-Luciferase Reporter Assay

After seeding 4×10^4 U2OS cells per well in 24-well plates, the cells were cotransfected with 200 ng NF-κB p65 luciferase reporter and 5 ng pRL-TK Renilla luciferase construct (Promega, Madison, WI) per well using Lipofectamine 2000 (Invitrogen). After 24 hours, the cells were treated with LiCl (20 mM) or siRNA (100 nM). Then, the cells were analyzed after an additional 48 hours according to the Dual-Luciferase Assay System protocol (Promega). For stable transfection, U2OS cells expressing constitutively active GSK-3β or empty vector (CA3, CA9, vec) or U2OS/MTX300 cells expressing kinase-inactive GSK-3β (SH4, SH35) were cotransfected with NF-κB p65 luciferase reporter and Renilla luciferase construct for 48 hours and then the cells were analyzed as described above.

Apoptosis Antibody Array

To study the mechanism of apoptosis induced by GSK-3β inhibition, the Proteome Profiler Human Apoptosis Array Kit (R&D Systems, Minneapolis, MN) was used according to manufacturer's instructions. Briefly, after blocking the arrays with array buffer, cell lysates were added and incubated overnight at 4°C. After extensive washes, the array was incubated with the antibody cocktail (antibodies to Bad, TRAILR1/DR4, PON2, Bax, TRAILR2/DR5, p21/CIP1/CDNK1A, Bcl-2, FADD, p27/Kip1, Bcl-x, Fas/TNFSF6, phospho-p53 [S15], pro-caspase-3, HIF-1α, phospho-p53 [S46], cleaved caspase-3, HO-1/HMOX1/HSP32, phospho-p53 [S392], catalase, HO-2/HMOX2, phospho-Rad17 [S635], cIAP-1, HSP27, SMAC/Diablo, cIAP-2, HSP60, survivin, claspin, HSP70, TNFRI/TNFRSF1A, clusterin, HTRA2/Omi, XIAP, cytochrome c, and livin) for 1 hour, washed with 1× wash buffer for 10 minutes and then incubated with streptavidin-HRP diluted as 1:5000 in 1× array buffer 2/3 for 30 minutes, followed by exposure to x-ray film.

Reverse Transcription-Polymerase Chain Reaction (RT-PCR)

Total cellular RNA was extracted from U2OS cells after siRNA transfection or LiCl treatment using the RNeasy Mini Kit (Qiagen, Hilden, Germany), and the first strand cDNA was synthesized by First Strand cDNA Synthesis Kit (Fermentas, Glen Burnie, MD), following the manufacturer's protocol. Primers included were the following: GSK-3β forward, 5′- ATTTCCAGGGGATAGTGG TGT-3′; GSK-3β reverse, 5′-GGTCGGAAGACCTTAGTC CAAG-3′; cIAP-1 forward, 5′- TTCCCAGGTCCCTCGTATCA AAA-3′; cIAP-1 reverse, 5′- TGGAGAAAGGCTGGAGTAAG AACC-3′; XIAP forward, 5′- TGGCACGAGCAGGGTTTC TTTA-3′; XIAP reverse, 5′- TGGGGTTAGGTGAGCATAGTC TGG-3′;Bcl2 forward. 5′ATGTGTGTGGAGAGCGTCAACC-3′; Bcl2 reverse, 5′- TGAGCAGAGTCTTCAGAGACAGCC-3′; survivin forward, 5′- GCCTGGCAGCCCTTTCTCAA-3′; survivin reverse, 5′- CTCGATGGCACGGCGCACTTTCT-3′; IκBα forward, 5′- CTCCGAGACTTTCGAGGAAATAC-3′; IκBα reverse, 5′- GCCATTGTAGTTGGTAGCCTTCA-3′; p65 forward, 5′- AGCTCAAGATCTGCCGAGTG-3′; p65 reverse, 5′- ACATCAGCTTGCGAAAAGGA-3′; β-actin forward, 5′- GT GGGGCGCCCCAGGCACCA-3′; β-actin reverse, 5′- CTCCT TAATGTCACGCACGATTTC-3′.

PCR was programmed as follows: 94°C for 2 minutes, 30 cycles of 94°C for 30 seconds, 54°C for 30 seconds, 72°C for 30 seconds, 72°C for 10 minutes, hold at 4°C. RT-PCR products were analyzed via 2.0% agarose gel electrophoresis and stained with ethidium bromide for visualization using ultraviolet light.

Western Blotting Analysis

Protein from U2OS cells treated with LiCl or transfected with siRNA or plasmids was extracted for western blotting as described previously (30,31). Sixty micrograms of total protein from each sample was loaded, resolved by electrophoresis in 8%–12% sodium dodecyl sulfate–polyacrylamide gradient gels, and transferred to nitrocellulose membranes. The blots were then incubated with various antibodies as described above. Pixel density was quantified with Quantity One (Bio-Rad, Hercules, CA).

Patients and Specimens

Patient studies were approved by the Institutional Review Board of Sun Yat-Sen University, and written informed consent was obtained from the patients or their parents before sample collection. In this study, osteosarcoma tissue samples were obtained from 74 patients, which included 25 primary biopsy samples and 49 samples from surgical resections. Biopsy samples were immediately fixed for 12–24 hours with 10% formaldehyde when they were obtained, and they were then paraffin embedded. Surgical resections were sent from the operating room to the pathology department within 1–2 hours after being excised. Afterward, the specimens were examined, photographed, and ultimately fixed with 10% formaldehyde within 3 hours after resection. The samples from all case patients were carefully examined following hematoxylin and eosin staining to confirm the diagnosis of osteosarcoma. These patients received standard neoadjuvant chemotherapy followed by resection of the tumor and postoperative chemotherapy at the Musculoskeletal Tumor Center of Sun Yat-Sen University (Guangzhou, People's Republic of China). Chemotherapy included methotrexate (MTX, 8–12 g/m^2), doxorubicin (ADM, 60–80 mg/m^2), cisplatin (DDP, 100–120 mg/m^2), or isofosfamide (IFO, 12.5 g/m^2). Of the 74 patients with osteosarcoma, 13 lacked follow-up records and the remaining 61 had a median follow-up of 4 years (ranging from 3 to 12.8 years); these data were used in survival analyses. Clinicopathologic features of the 61 patients are shown in Supplementary Table 1 (available online).

Immunohistochemical Staining

Immunohistochemical staining was performed, as described previously (31), on 3-μm sections from paraffin-embedded tissues of 74 patients with osteosarcoma. The primary antibodies against phosphorylated-GSK-3β (Serine 9) and p65 were diluted 1:50 and 1:100, respectively, and tissue sections were incubated with these antibodies at 4°C overnight in a humidified container. After washing with PBS three times, the tissue slides were treated with a non-biotin horseradish peroxidase detection system according to manufacturer's instructions (Dako, Carpinteria, CA). The results of immunohistochemical staining were evaluated by two independent pathologists, Dr A.-J. Han and Dr D.-W. Liu, who specialize in osteosarcoma. Samples were was classified as positive for phosphorylated-GSK-3β expression when there were more than 10% positive-staining cells and classified as negative otherwise (23). To evaluate nuclear NF-κB p65 localization, we searched for hot spots with nuclear staining and counted a total number of 500 nuclei within these hot spots at ×400 magnification (32,33). The sample was classified as positive for nuclear NF-κB p65 when more than 10% of the tumor cells on the slide showed nuclear staining overall. In the study, certain stained breast cancer tissues and prostate cancer tissues served as the positive controls for phosphorylated-GSK-3β and nuclear p65, respectively, whereas osteosarcoma specimens that were stained with the same concentration of rabbit IgG, without GSK-3β or NF-κB p65 antibodies, were used as negative controls.

Antitumor Assays Using Mouse Models

All in vivo experiments were approved by the Institutional Review Board of Sun Yat-Sen University. Athymic nude (nu/nu) mice, 6–8 weeks of age, were purchased from SLAC Animal Center (Shanghai, China). U2OS/MTX300 and ZOS cells (1×10^6 in 200 μL PBS) were injected subcutaneously near the scapula of the nude mice. One week after the cells were injected, the mice were randomly separated into groups that each contained six mice. The first two groups of mice were treated with LiCl (340 mg/kg) and/or PDTC (200 mg/kg) by intraperitoneal injection every 2 days. The remaining two groups of mice were treated with ADM (6 mg/kg) by intraperitoneal injection once per week and lithium carbonate (250 mg/kg) intragastrically every day. Tumors were measured with a caliper every 2 days, and the tumor volume was calculated using the formula $V = 1/2$ (width^2 × length). Body weights were also recorded. Mice were killed by cervical dislocation when the tumor diameters reached 1.5 cm, following the terms of the original protocol.

For orthotopic model of osteosarcoma, we used ZOS osteosarcoma cells, which had been derived from a primary tumor. The detailed procedure was described previously (34,35). Specifically, the mice were anesthetized by isoflurane, and their right legs were disinfected using 70% ethanol. A 30-gauge needle was carefully inserted into the proximal tibia through the cortex of the anterior tuberosity. Then, we confirmed that the needle was in the medullary cavity of proximal tibia by moving the needle forward and backward. Finally, 20 μL of the ZOS cell suspension was slowly injected. The syringe was flushed between injections. Eighteen days after injection of the cells, the mice were randomly separated into treatment groups (n = 5). Mice were treated with ADM (6 mg/kg) by intraperitoneal injection once per week and lithium carbonate (250 mg/kg) intragastrically every day. The length and width of tumors (D_1, D_2) were measured with a caliper every 2 days, and the tumor volume was calculated using the formula $V = 4/3\ \pi[1/4(D_1+D_2)]^2$, as described previously (34). Mice were killed by cervical dislocation when the tumor volume reached 500 mm^3 according to protocol filed with the Guidance of Institutional Animal Care and Use Committee of Sun Yat-Sen University.

Statistical Analysis

An unpaired Student's *t* test or analysis of variance with Bonferroni post hoc test (SPSS software 13.0; SPSS, Chicago, IL) was used for statistical comparison. The Kaplan-Meier method was used to estimate the overall survival, and the log-rank test was used to evaluate the differences between survival curves. Statistical tests and *P* values

were two-sided. *P* values that were less than .05 were considered to connote statistical significance.

Results

Association of Active GSK-3β With Clonogenicity and Tumorigenicity of Osteosarcoma Cell Lines

To determine the role of GSK-3β in osteosarcoma, we first examined the levels of GSK-3β that were phosphorylated at Serine 9, and thus known to be inactive (36), in five osteosarcoma cell lines and one normal osteoblast cell line. Normal osteoblast hFOB1.19 cells contained the highest level of p-Ser9-GSK-3β, whereas U2OS and SAOS osteosarcoma cells contained moderate levels of p-Ser9-GSK-3β (Figure 1, A). By contrast, MG63, ZOS, and ZOS-M osteosarcoma cells contained the lowest levels of p-Ser9-GSK-3β. However, total GSK-3β levels were comparable among these cell lines.

As expected based on previous findings (36), inactivation of GSK-3β indicated by accumulation of p-Ser9-GSK-3β in these osteosarcoma cell lines was associated with increased levels of β-catenin protein, which is an endogenous substrate of GSK-3β and thus expected to be expressed at lower levels if GSK-3β is active (Figure 1, B). p-Ser9-GSK-3β levels were also inversely related to the tumorigenicity of osteosarcoma cell lines as determined by colony formation in vitro. Cells with the lowest levels of p-Ser9-GSK-3β (ie, MG63, ZOS, and ZOS-M) formed more colonies than the cells with moderate levels of p-Ser9-GSK-3β (ie, U2OS and SAOS2); for example, at 14 days, the mean number of colonies from ZOS cells = 47, from U2OS cells = 15, difference = 32, 95% confidence interval (CI) = 11 to 52, *P* = .0017 (Figure 1, C).

To determine whether there was an association between GSK-3β activation and osteosarcoma tumor growth in vivo, each cell line was subcutaneously injected into five nude mice and tumor formation was followed for 5 weeks. No tumors were detected in mice injected subcutaneously with either U2OS or SAOS2 cells (Figure 1, D). By contrast, ZOS, ZOS-M, and MG63 cells were tumorigenic (at 56 days, all five mice had tumors from ZOS cells, all five mice had tumors from ZOS-M cells, and all five mice had tumors from MG63 cells). We also tested U2OS/MTX300 cells, a methotrexate-resistant variant derived from U2OS cells (21). U2OS/MTX300 cells formed more colonies than U2OS cells in vitro (at 14 days, the mean number of colonies from U2OS/MTX300 cells = 36, from U2OS cells = 15, difference = 21, 95% CI = 0.3 to 41, *P* = .045; Figure 1, C) and were more tumorigenic in vivo (at 56 days, all five mice had tumors with U2OS/MTX300 cells, and zero of five mice had tumors from U2OS cells; Figure 1, D). U2OS/MTX300 cells also had a much lower level of p-Ser9-GSK-3β than U2OS cells (Figure 1, E). Collectively, these results suggest that increased levels of GSK-3β activation (as measured by lack of p-Ser9-GSK-3β phosphorylation) are associated with greater tumorigenicity of osteosarcoma cells in vitro and in vivo.

Effect of Experimentally Modulated GSK-3β Activity on Clonogenicity and Tumorigenicity of Osteosarcoma Cells

To further confirm the finding that GSK-3β activity is associated with osteosarcoma tumorigenesis, we investigated whether alteration

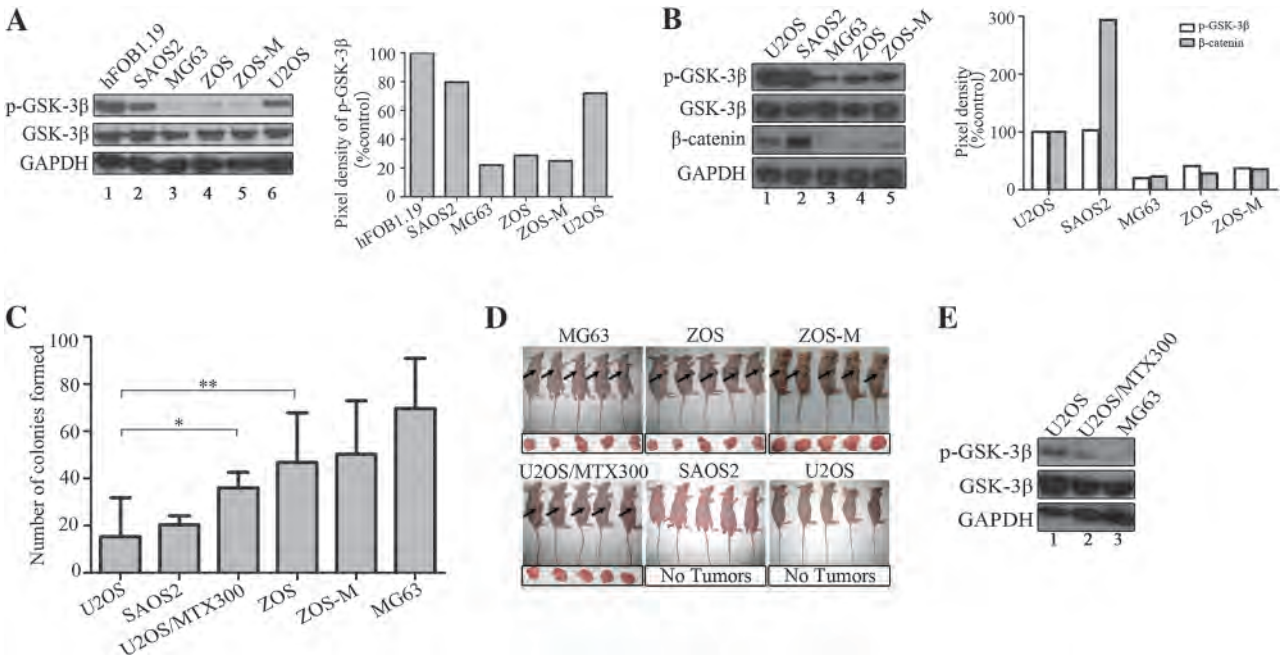

Figure 1. Glycogen synthase kinase-3β (GSK-3β) activity, clonogenicity of osteosarcoma cells in vitro, and tumorigenicity in vivo. **A**, **B**, **E**) Western blots showing levels of (inactive) phospho-Ser9-GSK-3β (p-GSK-3β) and of β-catenin in five osteosarcoma cell lines and one normal osteoblast line (hFOB1.19). The panels to the right of blots (**A**) and (**B**) show quantification of the pixel density of the GSK-3β and β-catenin bands in comparison to pixel density of a control, as indicated. **C**) Results of colony formation assays in which the indicated osteosarcoma cell lines were grown in six-well plates. Experiments were performed in triplicate; **error bars** refer to 95% confidence intervals; **P* = .045 and ***P* = .002. Two-sided analysis of variance with Bonferroni post hoc test was used. **D**) Tumorigenicity assay in which the indicated osteosarcoma cell lines were grown for 5 weeks in nude mice (n = 5 mice per group). Five of five mice developed a tumor when injected with ZOS cells, ZOS-M cells, or MG63 cells.

of the levels of active GSK-3β could modulate clonogenicity and tumorigenicity of osteosarcoma cell lines. In our first experiments, we used U2OS cells, which had moderate levels of p-Ser9-GSK-3β and did not form tumors in nude mice (Figure 1, A). We generated stable transfectants of U2OS cells that stably overexpressed a kinase-inactive (KD) form of GSK-3β, in which the lysine residue at the position 85 was substituted with alanine, or a CA form of GSK-3β, in which the serine residue at the position 9 was substituted with alanine (GSK-3β-S9A) (Figure 2, A). Stable transfectants were then single-cell cloned, to generate several lines of each cell type. Clonogenicity was substantially increased for CA3 and CA9, two cell lines in which GSK-3β was constitutively active, but not in KD2 and KD5, two cell lines in which GSK-3β was inactive, in comparison with the control U2OS cells (vec) that were stably transfected with empty vector (at 14 days, the mean number of colonies from CA3 cells = 39, from CA9 cells = 59, from vec cells = 25; difference, CA3 vs vec = 14, 95% CI = 0.43 to 28; $P = .042$; difference, CA9 vs vec = 34, 95% CI = 18 to 50, $P < .001$; Figure 2, B). Also, both CA3 and CA9 cells were tumorigenic in vivo, whereas there were no tumors detected in mice injected with KD2, KD5, or vec cells (at 56 days, three of five mice developed tumors from CA3 cells, five of five mice developed tumors from CA9 cells, and no mice developed tumors from vec cells; Figure 2, C). These results indicate that overexpression of active GSK-3β in an osteosarcoma cell line enhances clonogenicity in vitro and tumorigenesis in vivo.

In a second line of experimentation, we generated stable transfectants in which GSK-3β expression was silenced using a plasmid that expressed GSK-3β-specific shRNA. For these experiments, we chose U2OS/MTX300 cells, which had low p-Ser9-GSK-3β levels and a transformed phenotype both in vitro and in vivo. Again, stable transfectants were single-cell cloned to yield several cell lines. GSK-3β levels were reduced by 50% in two stable transfectants, SH4 and SH35 (Figure 3, A). Cell proliferation, as measured by growth curves (Figure 3, B), and clonogenicity, as measured by colony formation assays (Figure 3, C), also decreased by 50% in these cell lines compared with parental cells in which GSK-3β expression was not silenced (at 14 days, the mean number of colonies from SH4 cells = 18, from SH35 cells = 22, from vec cells = 41; difference, SH4 vs vec = -23, 95% CI = −32 to −15; $P < .001$; difference, SH35 vs vec = −19, 95% CI = −28 to −10, $P = .001$). Although both SH4 and SH35 cells were still tumorigenic in vivo, the tumors that arose in mice injected with these two transfectants were much smaller than those in mice that were injected with parental cells or with U2OS/MTX300 cells transfected with scrambled shRNA (at 25 days, the mean volume of tumors from SH4 cells = 177 mm^3, from SH35 cells = 128 mm^3, from vec cells = 411 mm^3; difference, SH4 vs vec = −234, 95% CI = −360 to −107; $P < .001$; difference, SH35 vs vec = −283, 95% CI = −409 to −156, $P < .001$; Figure 3, D–F). These results indicate that reduction of GSK-3β expression impairs clonogenicity and tumorigenicity of an osteosarcoma cell line. Taken together, our results indicate that GSK-3β activity is oncogenic in osteosarcoma cells.

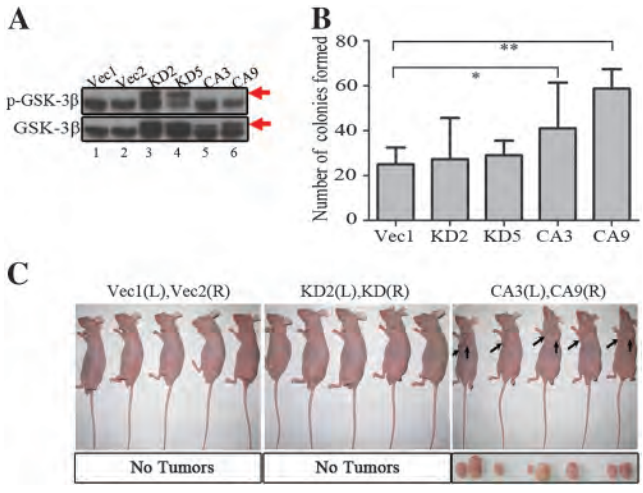

Figure 2. Clonogenicity and tumorigenicity of osteosarcoma cells that overexpress active glycogen synthase kinase-3β (GSK-3β). **A**) Western blot showing GSK-3β levels in U2OS cells stably transfected with the kinase-inactive form (KD2 and KD5) and the constitutively active form (CA3 and CA9) of GSK-3β, as well as empty vector (Vec1 and Vec2). **B**) Quantification of colony formation assay using the indicated stable transfectants. Experiments were performed in triplicate, and **error bars** refer to 95% confidence intervals. *$P = .042$ and **$P < .001$. Two-sided analysis of variance with Bonferroni post hoc test was used. **C**) Tumorigenicity of the indicated stable transfectants when grown for 5 weeks in the nude mouse model (n = 5 mice per group). Three of five mice that were injected with CA3 cells grew tumors, compared with five of five mice injected with CA9 cells, and none of the five mice injected with U2OS cells containing empty vector.

Effect of GSK-3β Inhibition on Osteosarcoma Cell Survival

Because expression of active GSK-3β had an oncogenic effect on osteosarcoma cells (Figures 1 and 2), we postulated that GSK-3β was critical for osteosarcoma cell survival. Indeed, cell proliferation was inhibited by LiCl, a known inhibitor of GSK-3β, in all osteosarcoma cell lines tested, including U2OS, U2OS/MTX300, MG63, SAOS2, ZOS, and ZOS-M cells (Figure 4, A and Supplementary Figure 1, available online). To rule out the possibility that decreased cell proliferation was a side effect mediated by LiCl treatment, these cells were also treated with two GSK-3β-specific inhibitors, GSK-3β inhibitor IX and SB216367. Both of these drugs also inhibited growth of osteosarcoma cells, including U2OS cells and ZOS cells (Figure 4, B). Consistent with these results, reduction of GSK-3β expression by GSK-3β-specific siRNA resulted in a 50% reduction in cell viability as measured by MTT assays (Figure 4, C). Furthermore, our previous findings that proliferation of U2OS/MTX300 cells was inhibited by stable expression of shRNA that reduced GSK-3β expression (Figure 3, B; SH4 and SH35) further confirmed the above findings with GSK-3β inhibitors and siRNA. These results indicate that GSK-3β is critical for cell proliferation in osteosarcoma cells.

Next, we sought to determine whether inhibition of GSK-3β would induce apoptosis in osteosarcoma cells. U2OS cells were treated with LiCl for several days, and western blots were used to measure GSK-3β activity (ie, absence of Serine 9 phosphorylation) and caspase 3 cleavage, a marker of apoptosis (Figure 4, D). Caspase 3 activity assays were also performed by extracting cellular protein from LiCl-treated U2OS cells and incubating caspase-3 substrate with a fixed amount of protein for 2 hours, followed by a colorimetric reading. Similar experiments were conducted with extracts from U2OS/MTX300 cells and from U2OS cells expressing CA or KD GSK-3β (Supplementary Figure 2, A, available online). LiCl

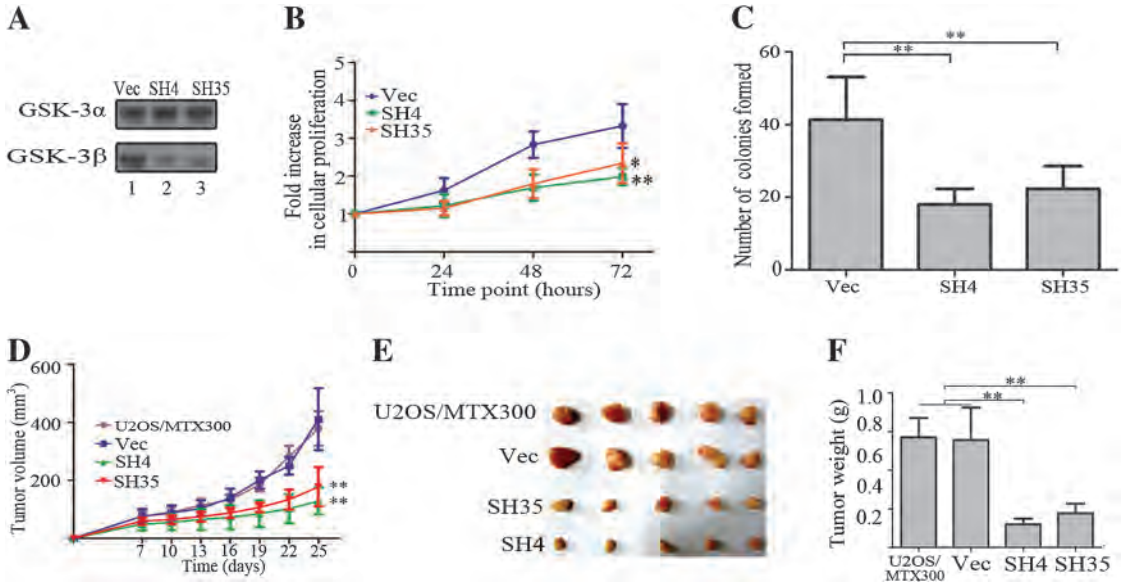

Figure 3. Effect of silencing glycogen synthase kinase-3β (GSK-3β) expression on clonogenicity and tumorigenicity of osteosarcoma cells. **A**) Western blot showing GSK-3β levels in SH4 and SH35 cells, which are U2OS/MTX300 cells stably transfected with GSK-3β-specific short hairpin RNA (shRNA). **B**) Growth curve of cells expressing GSK-3β shRNA as in (**A**). Experiments were performed in triplicate using the same cells as in (**A**), and **error bars** refer to 95% confidence intervals; *P = .002 and **P < .001 Two-sided analysis of variance (ANOVA) with Bonferroni post hoc test was used. **C**) Quantification of colony formation by cells expressing GSK-3β shRNA. Experiments were performed in triplicate using the same cells as in (**A**), and **error bars** refer to 95% confidence intervals; **P < .001. Two-sided ANOVA with Bonferroni post hoc test was used. **D**) Tumorigenicity assay of cells expressing GSK-3β shRNA. Experiments were carried out for 25 days using five mice per group, the same stable transfectants as in (**A**), and parental U2OS/MTX300 cells. Tumor volumes were monitored at day 7 and then every 3 days, as indicated. **Error bars** refer to 95% confidence intervals; **P < .001. Two-sided ANOVA with Bonferroni post hoc test was used. **E**) Xenografts excised from the tumor bearing mice in (**D**) at day 25. **F**) Weights of the xenografts from (**E**) at day 25. **Error bars** refer to 95% confidence intervals; **P < .001. Two-sided ANOVA with Bonferroni post hoc test was used.

treatment resulted in the suppression of GSK-3β activity in U2OS cells; p-Ser9-GSK-3β levels were increased by LiCl treatment (Figure 4, D and Supplementary Figure 2, A, available online). LiCl-mediated inhibition of GSK-3β also induced apoptosis in U20S and U2OS/MTX300 cells, as indicated by caspase-3 cleavage on western blots (Figure 4, D and Supplementary Figure 2, A, available online). Consistent with these results, caspase-3 activity assays also showed that inhibition of GSK-3β by LiCl or by GSK-3β-specific siRNA was accompanied by statistically significantly increased caspase-3 cleavage (eg, caspase-3 activity in U2OS cells treated for 72 hours with 20 mM LiCl = 2.97-fold compared with control, in untreated cells = 1 (referent); difference = 1.97-fold, 95% CI = 0.71- to 3.24-fold; P = .002; Figure 4, C and D, Supplementary Figure 2, A, available online). These results indicate that the activity of GSK-3β is critical for the cell survival of osteosarcoma cells because either silencing of GSK-3β expression or inhibition of GSK-3β activity using three different pharmacological inhibitors appeared to be able to induce apoptosis. GSK-3β inhibitors such as LiCl and GSK-3β inhibitor IX could reduce cell proliferation by inducing apoptosis in U2OS cells that expressed the kinase-inactive GSK-3 mutants (KD2 and KD5 cells) but not in U2OS cells that expressed constitutively active GSK-3β (CA3 and CA9 cells) (Figure 4, E, Supplementary Figure 2, B, available online, and data not shown). This finding suggested that this constitutively active mutant of GSK-3β was not sensitive to the inhibition mediated by LiCl and inhibitor IX. Taken together, these results indicate that GSK-3β is critical for cell survival in osteosarcoma.

GSK-3β as a Potential Therapeutic Target in Osteosarcoma

Because GSK-3β plays an important role in the survival of osteosarcoma cell lines (Figure 4 and Supplementary Figures 1 and 2, available online), we hypothesized that GSK-3β might be a potential therapeutic target in osteosarcoma. Because doxorubicin (ADM), methotrexate (MTX), and cisplatin (DDP) are commonly used chemotherapeutic drugs for patients with osteosarcoma in the clinic, we examined whether inhibition of GSK-3β would act additively with these chemotherapeutic drugs to kill osteosarcoma cells. U2OS cells were seeded in 96-well dishes and were simultaneously treated with LiCl (20 mM) and chemotherapy drugs (ADM 4 ng/mL, MTX 5 ng/mL, or DDP 200 ng/mL) for 72 hours. Cell viability was measured by MTT assay. GSK-3β inhibition by LiCl did enhance the apoptosis of U2OS or ZOS cells induced by ADM, MTX, or DDP in vitro (eg, for U2OS, the percentage of viable cells at 72 hours with 20 mM LiCl = 44%, with 4 ng/mL ADM = 75%, with both = 27%; difference, both vs ADM = 48%, 95% CI = 36% to 61%; P < .01; Figure 5, A and B and Supplementary Figure 3, A–D, available online). To further confirm the additive effect of GSK-3β inhibition with chemotherapeutic drugs, combinations of GSK-3β siRNA or other GSK-3β inhibitors and these chemotherapeutic drugs were tested. Silencing of GSK-3β expression also acted additively with ADM, MTX, and DDP to promote apoptosis of U2OS cells (Supplementary Figure 3, E–H, available online). Likewise, GSK-3β inhibition by GSK-3β inhibitor IX augmented the apoptosis of U2OS or ZOS cells induced by chemotherapeutic

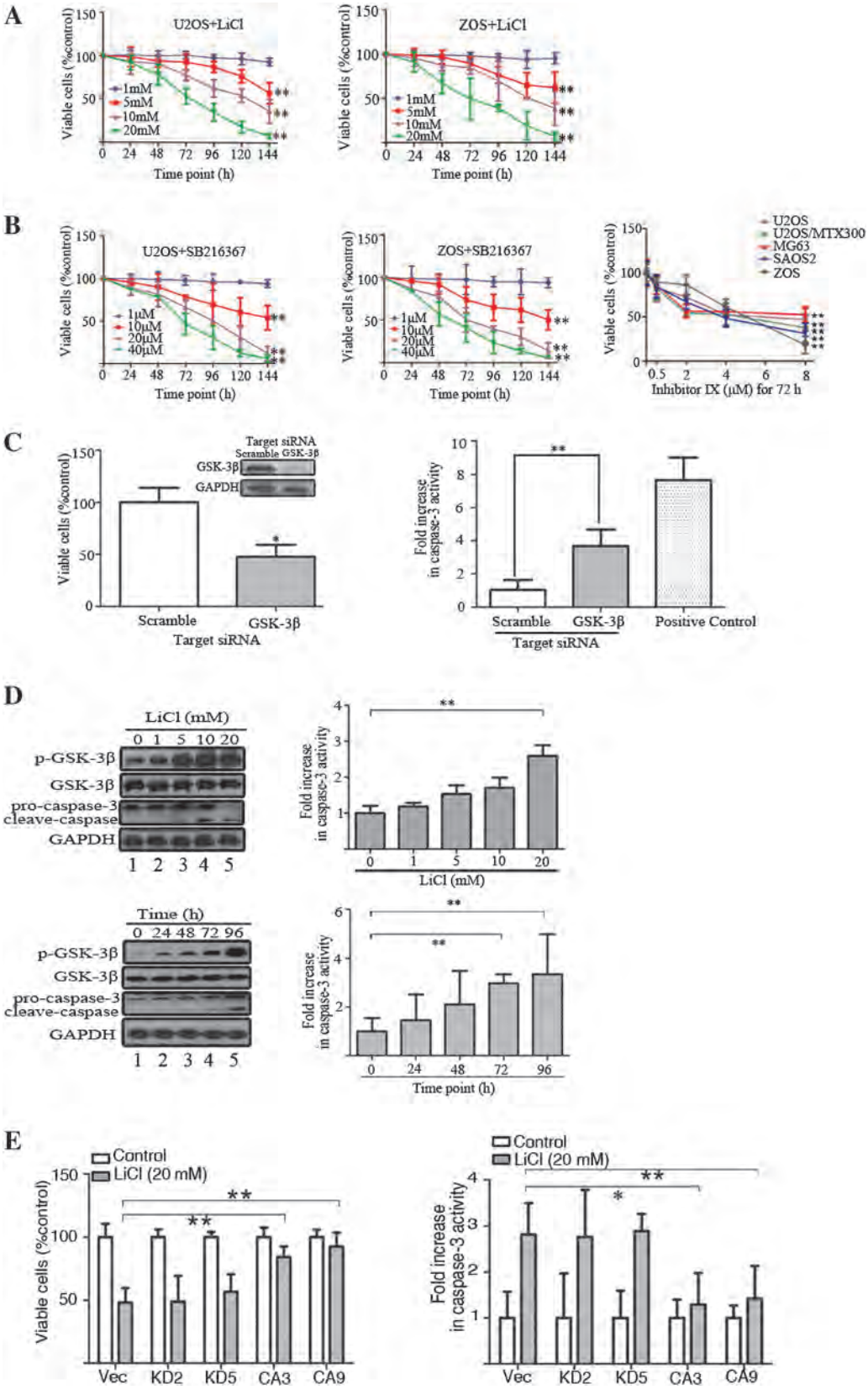

Figure 4. Glycogen synthase kinase-3β (GSK-3β) activity and cell survival among osteosarcoma cell lines. **A**) Viability of U2OS cells treated with LiCl, a GSK-3β inhibitor, as measured by 3-(4, 5-dimethylthiazol-2-yl)-2, 5-diphenyltetrazolium bromide (MTT) assays. Experiments were performed in triplicate; and error bars refer to 95% confidence intervals. $^{**}P < .001$. Two-sided analysis of variance (ANOVA) with Bonferroni post hoc test was used. **B**) Viability of U2OS and ZOS cells that were treated with SB216367 and inhibitor IX, both GSK-3β inhibitors, as measured by

(continued)

drugs, such as ADM, in vitro (Supplementary Figure 3, I, available online).

In another set of experiments, we examined the effect of GSK-3β inhibition on growth of osteosarcoma cells as xenografts in nude mice. For these experiments, U2OS/MTX300 or ZOS cells were injected into nude mice, and 1 week later, the mice were randomly separated into groups (Control, ADM, LiCl, and ADM + LiCl). ADM (6 mg/kg) was injected intraperitoneally once per week, and LiCl (340 mg/kg) was injected intraperitoneally every 2 days. Tumor measurements and body weights were recorded over the course of 3 weeks. Treatment with LiCl inhibited the growth of U2OS/MTX300 or ZOS cells as tumors in xenograft models (for U2OS/MTX300 xenografts at 17 days, the mean volume of tumors with no drugs = 1224 mm^3, with LiCl = 657 mm^3; difference = 567 mm^3, 95% CI = 127 to 1007; $P = .007$ mm^3; for ZOS xenografts at 21 days, the mean volume of tumors with no drugs = 1525 mm^3, with LiCl = 430 mm^3; difference = 1095 mm^3, 95% CI = 808 to 1384 mm^3; $P < .001$). Although the inhibitory effect of LiCl alone on tumor growth was comparable to that of ADM alone, ADM, but not LiCl, decreased mouse body weight, suggesting that LiCl treatment resulted in fewer side effects (Supplementary Figure 4, A and B, available online). More importantly, the combination of LiCl with ADM worked additively to inhibit tumor growth from osteosarcoma cells in nude mice (for U2OS/MTX300 xenografts at 17 days, the mean volume of tumors with ADM = 706.2 mm^3, with ADM + LiCl = 214.1 mm^3; difference = 492.1 mm^3, 95% CI = 74.1 to 910.1 mm^3; $P = .015$; for ZOS xenografts at 21 days, the mean volume of tumors with ADM = 457 mm^3, with ADM + LiCl = 127 mm^3; difference = 330 mm^3, 95% CI = 11 to 650 mm^3; $P = .044$). Because lithium carbonate is currently used in human patients with bipolar disorder, we also tested whether oral administration of lithium carbonate had a therapeutic effect on osteosarcoma using xenografts in a mouse model. Daily oral administration of lithium carbonate did synergize with ADM to enhance inhibition of the growth of tumors from U2OS/MTX300 osteosarcoma cells (Supplementary Figure 4, C–E, available online). To further evaluate the antitumor effect of lithium carbonate, we used an orthotopic model in which the ZOS osteosarcoma cell line was injected into the tibia of mice. Tumors were allowed to grow for 18 days, and the mice were then fed lithium carbonate (250 mg/kg). In these experiments, lithium carbonate inhibited tumor growth and acted additively with ADM (at 36 days, the mean volume of tumors with no drugs = 479 mm^3, with ADM = 143 mm^3, with LiCl = 187 mm^3, with both ADM and Li_2CO_3 = 80 mm^3; difference, no drugs vs Li_2CO_3 = 292 mm^3, 95% CI = 230 to 353 mm^3; $P < .001$; difference, ADM vs ADM + LiCl = 63 mm^3, 95% CI = 1.8 to 124.7 mm^3; $P = .041$; Figure 5, E and Supplementary Figure 5, available online). Our results indicate that GSK-3β inhibition enhances the therapeutic efficacy of these chemotherapeutic agents when used in combination to treat osteosarcoma.

Role of the NF-κB Pathway in GSK-3β-Mediated Osteosarcoma Cell Survival

Because GSK-3β inhibition induced apoptosis in osteosarcoma, we examined the effect of LiCl treatment on apoptosis-related proteins in U2OS cells using an antibody array. Although the expression of many proteins related to apoptosis was changed in U2OS cells treated with LiCl, we focused on proteins encoded by NF-κB target genes, including cIAP-1, xIAP, bcl2, and survivin, whose expression was inhibited by LiCl treatment. Expression of the NF-κB-regulated gene products cIAP-1, xIAP, bcl2, and survivin was inhibited by LiCl (Figure 6, A). These results were further confirmed by RT-PCR (Supplementary Figure 6, C, available online) and chromatin immunoprecipitation with anti-p65 antibody (Supplementary Figure 6, D, available online), indicating that the NF-κB pathway may be regulated by GSK-3β in osteosarcoma. In support of this conclusion, LiCl treatment of U2OS cells caused decreased IκBα phosphorylation, whereas the total protein level of IκBα was correspondingly increased (Figure 6, B). Likewise, nuclear localization of the NF-κB p65 protein, which is an indicator of NF-κB transcriptional activity, was also decreased in U2OS cells treated by LiCl (Figure 6, B). In addition, inhibition of GSK-3β by either LiCl or by GSK-3β-specific siRNA resulted in a substantial reduction of NF-κB-luciferase reporter activity (Figure 6, C). NF-κB-luciferase reporter activity was increased twofold in cell lines that expressed CA GSK-3β, but not in cell lines that expressed KD GSK-3β (Figure 6, D). By contrast, NF-κB-luciferase reporter activity was substantially decreased (by 50%) in SH4 and SH35 cells, which were stably transfected with GSK-3β-shRNA (Figure 6, D).

Next, we asked whether activation of the NF-κB pathway mediated the oncogenic effects of GSK-3β in osteosarcoma. Both the mutant form of IκBα [IκBα-mut, which is widely known to inhibit the NF-κB pathway (22)], and NF-κB p65-specific siRNA were able to enhance apoptosis of U2OS cells induced by LiCl (Figure 6, E). In addition, reduction of IκBα expression by siRNA in U2OS cells partially reversed the inhibitory effect of LiCl on cell viability (Figure 6, F). Likewise, cells ectopically transfected

Figure 4 (continued).

MTT assays. Experiments were performed in triplicate; and **error bars** refer to 95% confidence intervals; $**P < .001$. Two-sided ANOVA with Bonferroni post hoc test was used. **C**) Effect of GSK-3β silencing on apoptosis of osteosarcoma cells. U2OS cells were treated with control short interfering RNA (siRNA) or GSK-3β-specific siRNA for 72 hours and cellular viability was monitored by MTT assays (left panel, $P = .019$), and caspase-3 activity was also measured (right panels, $P < .001$). An unpaired two-sided Student's *t* test was used. Experiments were performed in triplicate; and **error bars** refer to 95% confidence intervals. **D**) Effect of GSK-3β inhibition on apoptosis of osteosarcoma cells. U2OS cells were treated with 1–20 mM LiCl for 72 hours (upper panel), or with 20 mM LiCl for 24–96 hours (lower panel) as indicated. Caspase 3 cleavage was determined by western blotting (left panels, $P = .007$), and caspase-3 activity assays were performed (right panels, $P < .001$). Two-sided ANOVA with Bonferroni post hoc test was used. Experiments were performed in triplicate; and **error bars** refer to 95% confidence intervals. **E**) Effect of LiCl treatment on osteosarcoma cells with varying levels of active GSK-3β. U2OS cells stably transfected with the kinase-inactive form (KD2 and KD5) and the constitutively active form (CA3 and CA9) of GSK-3β (shown in Figure 2, A) were treated with 20 mM LiCl for 72 hours or were left untreated, and then cell viability was monitored by the MTT assay (left panel, $**P < .001$), and caspase-3 activity was measured (right panel, $*P = .016$, $**P < .001$). Two-sided ANOVA with Bonferroni post hoc test was used. Experiments were performed in triplicate; and **error bars** refer to 95% confidence intervals.

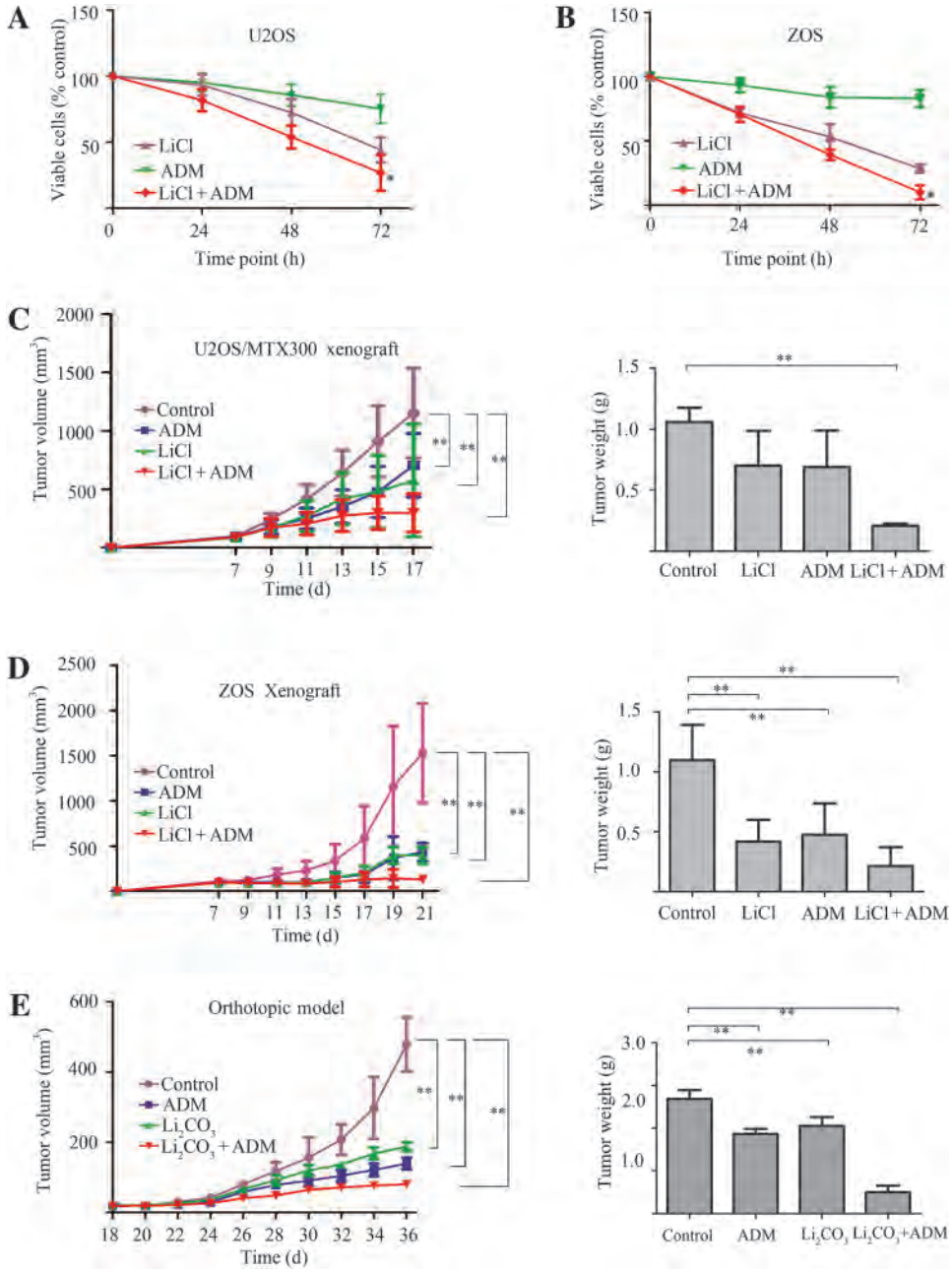

Figure 5. Glycogen synthase kinase-3β (GSK-3β) as a potential therapeutic target in osteosarcoma, in vitro and in vivo. (**A**, **B**) Effect of LiCl/doxorubicin (ADM) combination treatments on osteosarcoma cells in vitro. U2OS or ZOS cells were treated with LiCl (20 mM), ADM (4 ng/mL), or both for 72 hours, as indicated. Cell viability was measured by 3-(4,5-dimethylthiazol-2-yl)-2, 5-diphenyltetrazolium bromide (MTT) assays. Experiments were performed in triplicate; and **error bars** refer to 95% confidence intervals. **P* = .011 for (**A**) and * *P* = .021 for (**B**). Two-sided analysis of variance (ANOVA) with Bonferroni post hoc test was used. **C** and **D**) Effect of LiCl and/or ADM combination treatments on osteosarcoma xenografts in nude mice. U2OS/MTX300 or ZOS cells were injected subcutaneously in nude mice (n = 6 per group), and tumors were allowed to grow for 17 or 21 days. Starting on day 7, the mice were given LiCl (340 mg/kg) every 2 days and/or ADM (6 mg/kg) once a week intraperitoneally. The tumor volumes were monitored on day 7 and then every 2 days, as indicated (left panels), and the xenografts were excised and weighed on day 17 (right panels). **Error bars** refer to 95% confidence intervals. ***P* < .001. Two-sided ANOVA with Bonferroni post hoc test was used. **E**) Use of lithium carbonate and ADM to treat osteosarcoma in an orthotopic mouse model. ZOS cells were implanted in the proximal tibia and allowed to grow for 36 days. Starting on day 18, mice (n = 5 per group) were administered 250 mg/kg lithium carbonate intragastrically every day and/or 6 mg/kg ADM intraperitoneally once a week. The tumor volumes were monitored at day 18 and then every 2 days, as indicated (left panels), and the xenografts were then excised and weighed on day 36 (right panels). **Error bars** refer to 95% confidence intervals; ***P* < .001. Two-sided ANOVA with Bonferroni post hoc test was used.

with p65 were more resistant to apoptosis by LiCl (Figure 6, F). Taken together, these results demonstrate that GSK-3β activation stimulates NF-κB activity and that inhibition of the NF-κB pathway induces apoptosis in osteosarcoma cells.

Combined Effect of LiCl, Chemotherapeutic Drugs, and NF-κB Inhibitors on Osteosarcoma Growth

Because GSK-3β regulates cell survival partially through the NF-κB pathway in osteosarcoma cell lines and because NF-κB

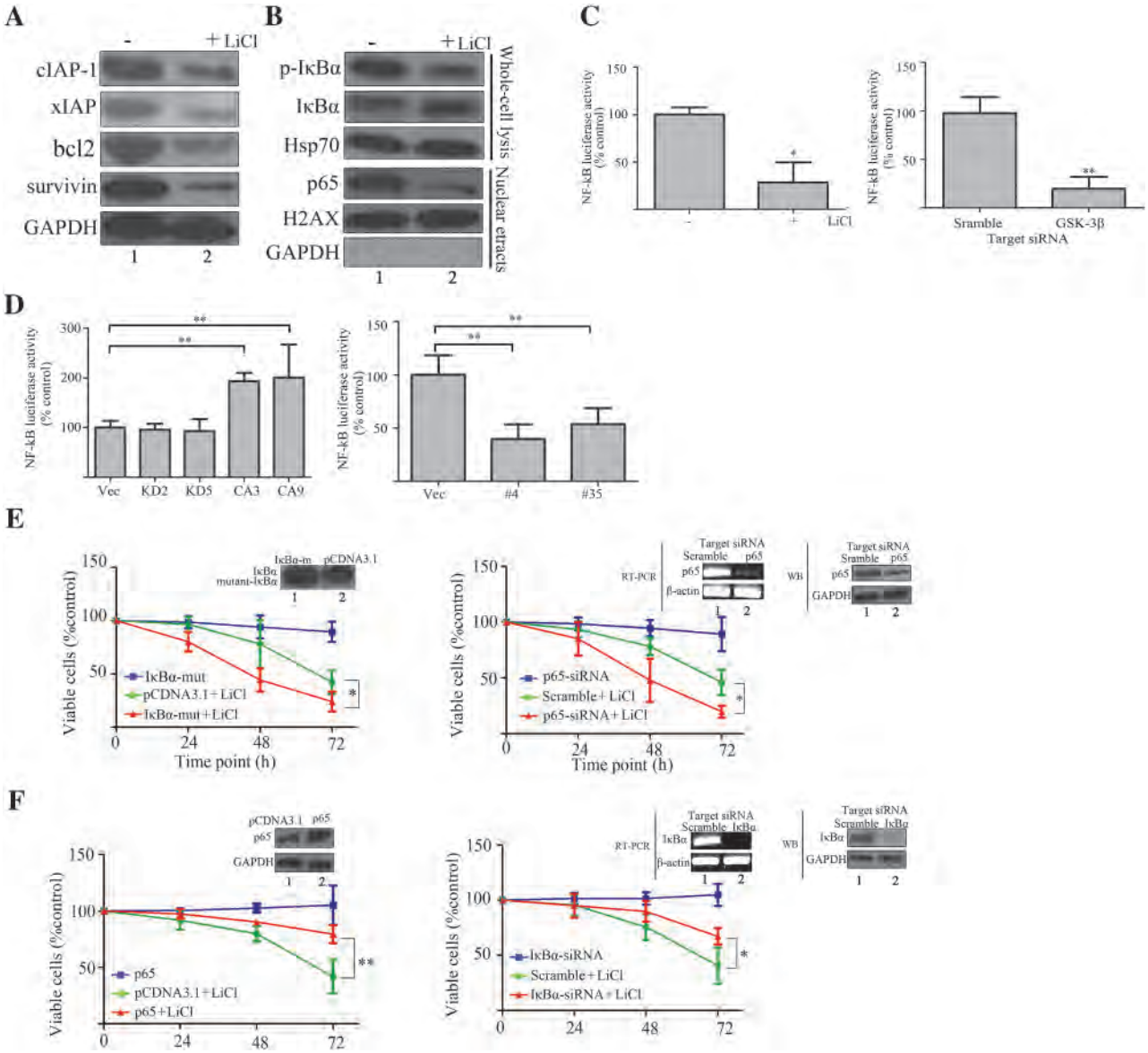

Figure 6. A role for the nuclear factor-κB (NF-κB) pathway in glycogen synthase kinase-3β (GSK-3β)–regulated osteosarcoma cell survival. **A** and **B**) Effect of GSK-3β inhibition on NF-κB pathway-related and apoptosis-related protein expression. U2OS cells were treated with 20 mM LiCl for 72 hours or left untreated, and the indicated proteins were analyzed by western blotting. **C**) Effect of GSK-3β inhibition on NF-κB-mediated transcription. U2OS cells were transfected with a plasmid encoding a luciferase reporter protein under NF-κB-mediated transcriptional control, and they were then treated with or without LiCl (20 mM) (left panel, $*P = .018$), or control or GSK-3β-siRNA (right panel, $**P < .001$) for 72 hours. The NF-κB luciferase activity was monitored as described in the "Methods" section. Experiments were performed in triplicate; **error bars** refer to 95% confidence intervals. An unpaired two-sided Student's *t* test was used. **D**) Effect of varying GSK-3β levels on NF-κB-mediated transcription. Stably transfected U2OS or U2OS/MTX300 cells (as shown in Figures 2 and 3) were transfected with the NF-κB-luciferase reporter and NF-κB-regulated luciferase activity was monitored as described in the "Methods" section. Experiments were performed in triplicate; **error bars** refer to 95% confidence intervals; $**P < .001$. Two-sided analysis of variance (ANOVA) with Bonferroni post hoc test was used. **E** and **F**) Viability of osteosarcoma cells in the presence of a mutant IκBα protein that inhibits the NF-κB pathway. Cellular viability assays were performed in U2OS cells transiently transfected with plasmids encoding the mutant form of IκBα (IκBα-mut; in which two serine residues at both 32 and 36 were changed into alanine residues), NF-κB p65-siRNA, IκBα-siRNA, or NF-κB p65 for 72 hours. The inserts show western blotting (WB) and reverse transcription-polymerase chain reaction experiments to quantify the expression of the transfected genes. Experiments were performed in triplicate; **error bars** refer to 95% confidence intervals; $*P = .0045$ in left panel and $*P = .001$ in the right panel for (**E**); $**P < .001$ in left panel and $*P = .001$ in the right panel for (**F**). Two-sided ANOVA with Bonferroni post hoc test was used. RT-PCR = reverse transcription-polymerase chain reaction.

inhibitors such as pyrrolidine dithiocarbamate (PDTC), parthenolide (PARTH), and Bay 11-7085 (BAY) have been successfully used in preclinical studies in mouse models (4,37–39), we investigated whether apoptosis could be increased by the inhibition of both NF-κB and GSK-3β in osteosarcoma. U2OS and ZOS osteosarcoma cells were seeded in 96-well dishes and treated with different concentrations of LiCl (20 mM), chemotherapy drugs (ADM 4 ng/mL, MTX 5 ng/mL, DDP 200 ng/mL) and/or NF-kB inhibitors (PDTC 10 μM, PARTH 2 μM, BAY 2.5 μM) for 48 hours, and cell viability was measured by MTT assay. As expected, treatment with

LiCl or NF-κB inhibitors could induce apoptosis in both ZOS and U2OS cells (Figure 7, A, Supplementary Figure 7, A and B, available online). More importantly, the combination of LiCl with several different NF-κB inhibitors enhanced the induction of apoptosis in these two cell lines. Because GSK-3β inhibition resulted in the chemotherapeutic enhancement in osteosarcoma (Figure 5 and Supplementary Figure 3, available online) and DNA damage induced by chemotherapeutic drugs often also results in NF-κB pathway–dependent apoptosis (16), we next tested combinations of LiCl, ADM, and NF-κB inhibitors to treat osteosarcoma. Combinations of LiCl, ADM, and NF-κB inhibitors induced more apoptosis than either LiCl with ADM or LiCl with NF-κB inhibitors in U2OS or ZOS cells in vitro (eg, for U2OS cells, the percentage of viable cells with LiCl = 75%, with LiCl + ADM = 52%, with LiCl + PDTC= 35%, with LiCl + ADM + PDTC = 12%; difference, LiCl vs Li + ADM = 22%, 95% CI = 0.83% to 43%; $P = 0.038$; difference, LiCl vs all three drugs = 63%, 95% CI = 41% to 84%; $P < .001$; Figure 7, A, Supplementary Figure 7, A and B, available online). Most importantly the combination of LiCl with either ADM or PDTC was more effective than LiCl alone for inhibiting tumor growth in mice carrying xenografts of ZOS cells, and the combination of LiCl, ADM, and PDTC showed the most statistically significant inhibition of tumor growth (at 21 days, mean tumor volume with LiCl = 443 mm^3, with LiCl + ADM = 175 mm^3, with LiCl + PDTC= 210 mm^3, with LiCl + ADM + PDTC = 124 mm^3; difference, LiCl vs Li + ADM = 269 mm^3, 95% CI = 118 to 420 mm^3; $P < .001$; difference, LiCl vs all three drugs = 319 mm^3, 95% CI = 167 to 469 mm^3; $P < .001$; Figure 7, B–D). Notably, the inhibitory effect of PDTC on tumor growth was comparable to that of ADM or LiCl alone, and like LiCl, PDTC had minimal toxicity in vivo, as indicated by mouse body weight (Figure 7, E). Collectively, these results indicate that the combination of LiCl, ADM, and NF-κB inhibitors may be an attractive therapeutic modality for treating osteosarcoma.

Association of GSK-3β Activity with Clinical Outcome Among Osteosarcoma Patients

We also determined whether GSK-3β activity was associated with the clinical outcome of patients with osteosarcoma. To this end, tumor samples from 74 osteosarcoma patients were collected for immunohistochemistry using anti-p-Ser9-GSK-3β and anti-p65 antibodies. Among them, 33 patients' samples (40%, including 10 biopsy samples and 23 surgical resections) were positive for p-Ser9-GSK-3β (indicating GSK-3β inhibition), whereas 41 patients' samples (60%, including 15 biopsy samples and 26 surgical resections) were negative for p-Ser9-GSK-3β, with breast cancer tissues as the positive control (Supplementary Figure 8, A and B, available online). These results demonstrated hyperactivation of GSK-3β in

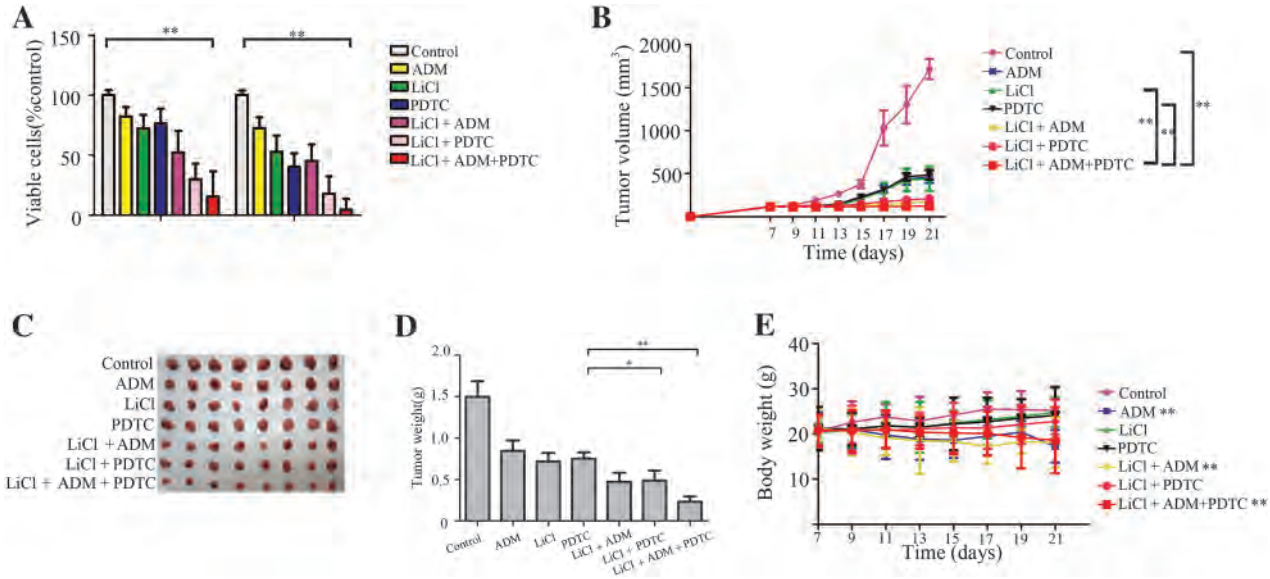

Figure 7. Combination of LiCl, doxorubicin (ADM), and nuclear factor-κB (NF-κB) inhibitors to target osteosarcoma in vitro and in vivo. **A**) Viability of osteosarcoma cells treated with LiCl, ADM, and/or an NF-κB inhibitor. U2OS or ZOS cells were treated with ADM (4 ng/mL), LiCl (20 mM), and/or pyrrolidinedithiocarbamate (PDTC; 10 μM), as indicated, for 48 hours. Cell viability was measured by 3-(4, 5-dimethylthiazol-2-yl)-2, 5-diphenyltetrazolium bromide (MTT) assays. Experiments were performed in triplicate; **error bars** refer to 95% confidence intervals; $^{**}P < .001$. Two-sided analysis of variance (ANOVA) with Bonferroni post hoc test was used. **B**) Size of osteosarcoma xenografts in mice treated with LiCl, ADM, and/or an NF-κB inhibitor. ZOS cells were injected subcutaneously into right flank of nude mice and allowed to grow for 21 days. Starting on day 7, mice (n = 8 per group) were administered 340 mg/kg LiCl every 2 days and/or 6 mg/kg ADM once a week and/or 200 mg/kg PDTC every 2 days intraperitoneally, and the tumor volumes were monitored at day 7 and then every 2 days, as indicated. **Error bars** refer to 95% confidence intervals. Means with 95% confidence intervals for each group are as follows: Control = 1715 mm^3 (95% CI = 1598 to 1832); ADM = 465 mm^3 (95% CI = 393 to 537); LiCl = 443 mm^3 (95% CI = 300 to 587); PDTC = 488.2 mm^3 (95% CI = 430 to 546); LiCl + ADM = 175 mm^3 (95% CI = 154 to 195); LiCl + PDTC = 211 mm^3 (95% CI = 197 to 224); LiCl + ADM + PDTC = 124.7 mm^3 (95% CI = 113 to 136); $^{**}P < .001$. **C** and **D**) Gradient of tumor sizes in mice treated with LiCl, ADM, and/or an NF-κB inhibitor. The xenografts were excised from the mice in panel (**B**) on day 21 and were photographed as shown in panel (**C**). They were then weighed, as shown in panel (**D**). **Error bars** refer to 95% confidence intervals; $^{*}P = .011$ and $^{**}P < .001$. Two-sided ANOVA with Bonferroni post hoc test was used. **E**) Effect of drug treatments on mouse body weights, as an indicator of toxicity. Body weights of the mice bearing xenografts in (**B**) were measured every 2 days as indicated. **Error bars** refer to 95% confidence intervals. $^{**}P < .001$. Two-sided ANOVA with Bonferroni post hoc test was used.

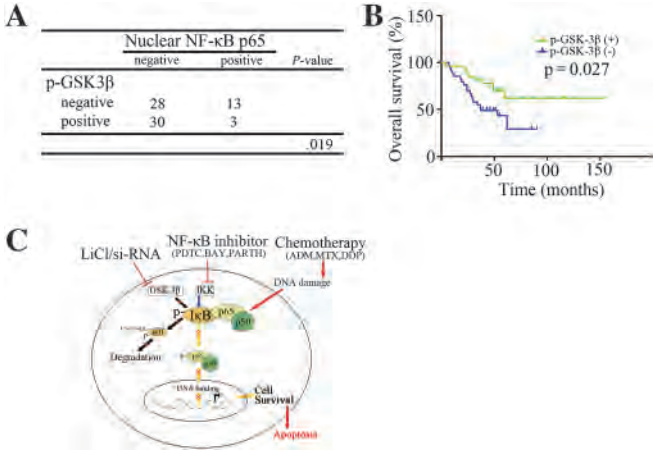

Figure 8. Association of glycogen synthase kinase-3β (GSK-3β) activity with the clinical outcome of patients with osteosarcoma. Immunohistochemical analysis was performed on 3-μm sections from paraffin-embedded tissues of 74 patients with osteosarcoma using the primary antibodies against phosphorylated-GSK-3β (Serine 9) or p65, as described in "Materials and Methods." An inverse relationship was observed between (inactive) p-Ser9-GSK-3β and (active) nuclear p65 levels in osteosarcoma samples in the clinic; $P = .019$. **B**) Overall survival rates of patients with osteosarcoma positive or negative for p-Ser9-GSK-3β were estimated with the Kaplan–Meier method by log-rank test; n = 61, $P = .027$. **C**) Proposed model. The nuclear factor-κB (NF-κB) pathway may have critical roles in the cell survival of osteosarcoma, which are mainly mediated by GSK-3β and IκB kinase (IKK). When GSK-3β or IKK is impeded, IκBα is stabilized and retained in the cytoplasm, causing the cell survival pathway to be impaired directly, which in turn enhances apoptosis induced by chemotherapies for osteosarcoma.

the majority of patients with osteosarcoma. More interestingly, 16 patients' samples were positive for nuclear localization of NF-κB p65 (seven biopsy samples and nine surgical sections), whereas 58 patients' samples were negative (18 biopsy samples and 40 surgical resections). These results suggested that inactive p-Ser9-GSK-3β is associated with osteosarcoma ($P = .019$; Figure 8, A) and indicate that the GSK-3β/NF-κB pathway is affected in patients with osteosarcoma. Among 74 patients with osteosarcoma, 61 patients, whose characteristics are listed in Supplementary Table 1 and Supplementary Methods (available online), were successfully followed up, and most of them had tumors that were grade IIB according to the Enneking staging system (40). Among these 61 patients, there was a statistically significant difference in overall survival between the 27 patients whose tumors were positive for (inactive) p-Ser9-GSK-3β and the 34 patients whose tumors were negative for (inactive) p-Ser9-GSK-3β as estimated with the Kaplan–Meier method by log-rank test (at a median follow-up of 4 years, OS for patients whose tumors had inactive GSK-3β = 109.2 months, OS for patients whose tumors did not have inactive GSK-3β = 49.2 months, $P = .027$; Figure 8, B). Our results indicate that increased expression of active GSK-3β is associated with poor prognosis in patients with osteosarcoma.

Discussion

In this report, we demonstrated that GSK-3β activity is positively associated with clonogenicity and tumorigenicity and is critical for cell survival in osteosarcoma. Inhibition of GSK-3β partially decreased the expression of NF-κB pathway genes and yielded antitumor effects in mouse models of osteosarcoma. We conclude that GSK-3β positively regulates the NF-κB pathway to promote oncogenic activities in osteosarcoma and that therapeutic targeting of the GSK-3β and/or NF-κB pathways may be a promising strategy to enhance the therapeutic activity of anticancer drugs against osteosarcoma in vitro and in vivo.

GSK-3β, a key component of both the canonical WNT/β-catenin and PI3K/Akt signaling pathways, is commonly considered a tumor suppressor in multiple cancers, such as breast and skin cancer (7). In this set of cancers, inhibition of GSK-3β favors cell proliferation and tumorigenesis (5,7,9). On the other hand, GSK-3β was found to function as an oncogene in several cancer types, such as mixed lineage leukemia (8–10), glioma (11), and oral cancer (7). In these cancers, inhibition of GSK-3β may serve as a therapeutic target (5,7,9). Here, we provide evidence that GSK-3β positively regulates the NF-κB pathway and is a promising therapeutic target in osteosarcoma, especially if GSK-3β inhibition is combined with ADM and/or NF-kB inhibitors. Because both LiCl (Figure 5 and 7) and lithium carbonate (Figure 5, E, Supplementary Figures 4, C and D and 5, available online) had a therapeutic effect and low toxicities were observed, targeting GSK-3β in patients with osteosarcoma may represent a novel and feasible approach. Of these, lithium carbonate carries the extra advantage that it is already currently in clinical use for patients with bipolar disorder. In addition, GSK-3β inactivation (p-Ser9-GSK-3β) may represent a valuable biomarker for predicting prognosis; the status of the GSK-3β/NF-κB pathway may have the potential to guide personalized therapies in the future by directing subsets of osteosarcoma patients to therapies that target GSK-3β and NF-κB signaling, such as combinations of ADM, lithium carbonate, and/or NF-kB inhibitors.

The NF-κB pathway is activated by a variety of cellular and developmental signals (12–15). Deregulated activation of NF-κB has been observed and causally linked to tumor chemoresistance (16). Here, we showed that NF-kB inhibitors could suppress the growth of osteosarcoma and that GSK-3β inhibition could enhance this effect both in vitro and in vivo. We also showed that GSK-3β–induced activation of NF-kB pathway may cause chemoresistance in osteosarcoma tumors.

Biological and pathological functions of GSK-3β have been linked to the NF-κB pathway for a decade (41), but the question of how GSK-3β activates NF-κB signaling is poorly understood. In pancreatic cancer, GSK-3α/β maintains constitutive NF-κB activation by regulating IκB kinase (IKK) activity and the loss of GSK-3α/β blocks IκBα phosphorylation (42). However, in GSK-3β-deficient mouse embryonic fibroblasts, degradation of IκBα and translocation of NF-κB to the nucleus were unaffected (41). We may speculate that GSK-3β may phosphorylate IκBα to release p65 and p50 into the nucleus to affect target gene expression because IκBα may be phosphorylated by GSK-3β, as previously proposed (43). In addition, GSK-3β may phosphorylate p65 to enhance the transcriptional activity of p65, as shown in pancreatic cancer (42). Considering the established role of IKK in NF-κB pathway, we propose that the NF-κB pathway may have critical roles in the cell survival of osteosarcoma, which are mainly mediated by GSK-3β and IKK (Figure 8, C). When GSK-3β or IKK is

impeded, IκBα is stabilized and retained in the cytoplasm, and the cell survival pathway is impaired directly. This may explain why GSK-3β inhibition acted additively with NF-kB inhibitors for osteosarcoma in vitro and in vivo.

In addition, as shown in some cancer cells (44), chemotherapies, including ADM and DDP, are able to induce apoptosis through the NF-kB pathway. This may explain why chemotherapies, such as ADM, MTX, and DDP, could be enhanced by GSK-3β inhibition and/or NF-kB inhibitors for osteosarcoma in vitro and in vivo. However, further investigation is required to fully elucidate how NF-κB activity is regulated by GSK-3β in osteosarcoma. Villalobos et al. (45) recently identified GSK-3β consensus sequences in IkB that impact ligand-induced IkB processing and NF-kB signaling. This finding may directly support our model for osteosarcoma.

There are several limitations to our work. First, we did not determine the exact mechanism through which GSK-3β regulates NF-κB signaling, and this deserves to be further investigated. Second, our results were obtained from osteosarcoma cell lines grown as xenografts in nude mice, and the real situation in the patients with osteosarcoma may be different. Therefore, we look forward to the results of clinical trials to test combinations of chemotherapy drugs with lithium carbonate and/or NF-κB inhibitors in patients with osteosarcoma.

In summary, we have clearly demonstrated that GSK-3β represents a promising therapeutic target in osteosarcoma. More importantly, patients with osteosarcoma may be treated individually in the future, depending on the status of the GSK-3β–NF-κB pathway.

References

1. Biermann JS, Adkins D, Benjamin R, et al. Bone cancer. *J Natl Compr Canc Netw.* 2007;5(4):420–437.
2. Gorlick R, Anderson P, Andrulis I, et al. Biology of childhood osteogenic sarcoma and potential targets for therapeutic development: meeting summary. *Clin Cancer Res.* 2003;9(15):5442–5453.
3. Siegel HJ, Pressey JG. Current concepts on the surgical and medical management of osteosarcoma. *Expert Rev Anticancer Ther.* 2008;8(8):1257–1269.
4. Watson RL, Spalding AC, Zielske SP, et al. GSK3beta and beta-catenin modulate radiation cytotoxicity in pancreatic cancer. *Neoplasia.* 2010;12(5):357–365.
5. Cohen P, Frame S. The renaissance of GSK3. *Nat Rev Mol Cell Biol.* 2001;2(10):769–776.
6. Doble BW, Woodgett JR. GSK-3: tricks of the trade for a multi-tasking kinase. *J Cell Sci.* 2003;116(pt 7):1175–1186.
7. Mishra R. Glycogen synthase kinase 3 beta: can it be a target for oral cancer. *Mol Cancer.* 2010;9(1):144.
8. Zou CY, Wang J, Shen JN, et al. Establishment and characteristics of two syngeneic human osteosarcoma cell lines from primary tumor and skip metastases. *Acta Pharmacol Sin.* 2008;29(3):325–332.
9. Patel S, Woodgett J. Glycogen synthase kinase-3 and cancer: good cop, bad cop? *Cancer Cell.* 2008;14(5):351–353.
10. Wang XQ, Ongkeko WM, Chen L, et al. Octamer 4 (Oct4) mediates chemotherapeutic drug resistance in liver cancer cells through a potential Oct4-AKT-ATP-binding cassette G2 pathway. *Hepatology.* 2010;52(2):528–539.
11. Kotliarova S, Pastorino S, Kovell LC, et al. Glycogen synthase kinase-3 inhibition induces glioma cell death through c-MYC, nuclear factor-kappaB, and glucose regulation. *Cancer Res.* 2008;68(16):6643–6651.
12. Ghosh S, Karin M. Missing pieces in the NF-kappaB puzzle. *Cell.* 2002;109(suppl):S81–S96.
13. Karin M, Ben-Neriah Y. Phosphorylation meets ubiquitination: the control of NF-[kappa]B activity. *Annu Rev Immunol.* 2000;18:621–663.
14. Silverman N, Maniatis T. NF-kappaB signaling pathways in mammalian and insect innate immunity. *Genes Dev.* 2001;15(18):2321–2342.
15. Sasaki Y, Schmidt-Supprian M, Derudder E, Rajewsky K. Role of NFkappaB signaling in normal and malignant B cell development. *Adv Exp Med Biol.* 2007;596:149–154.
16. Wang CY, Cusack JC Jr, Liu R, Baldwin AS Jr. Control of inducible chemoresistance: enhanced anti-tumor therapy through increased apoptosis by inhibition of NF-kappaB. *Nat Med.* 1999;5(4):412–417.
17. Higgins KA, Perez JR, Coleman TA, et al. Antisense inhibition of the p65 subunit of NF-kappa B blocks tumorigenicity and causes tumor regression. *Proc Natl Acad Sci U S A.* 1993;90(21):9901–9905.
18. Eliseev RA, Zuscik MJ, Schwarz EM, O'Keefe RJ, Drissi H, Rosier RN. Increased radiation-induced apoptosis of Saos2 cells via inhibition of NFkappaB: a role for c-Jun N-terminal kinase. *J Cell Biochem.* 2005;96(6):1262–1273.
19. Andela VB, Schwarz EM, Puzas JE, O'Keefe RJ, Rosier RN. Tumor metastasis and the reciprocal regulation of prometastatic and antimetastatic factors by nuclear factor kappaB. *Cancer Res.* 2000;60(23):6557–6562.
20. Eliseev RA, Schwarz EM, Zuscik MJ, O'Keefe RJ, Drissi H, Rosier RN. Smad7 mediates inhibition of Saos2 osteosarcoma cell differentiation by NFkappaB. *Exp Cell Res.* 2006;312(1):40–50.
21. Yin JQ, Shen JN, Su WW, et al. Bufalin induces apoptosis in human osteosarcoma U-2OS and U-2OS methotrexate300-resistant cell lines. *Acta Pharmacol Sin.* 2007;28(5):712–720.
22. Deng J, Miller SA, Wang HY, et al. beta-catenin interacts with and inhibits NF-kappa B in human colon and breast cancer. *Cancer Cell.* 2002;2(4):323–334.
23. Kang T, Wei Y, Honaker Y, et al. GSK-3 beta targets Cdc25A for ubiquitin-mediated proteolysis, and GSK-3 beta inactivation correlates with Cdc25A overproduction in human cancers. *Cancer Cell.* 2008;13(1):36–47.
24. Liu SF, Ye X, Malik AB. Inhibition of NF-kappaB activation by pyrrolidine dithiocarbamate prevents in vivo expression of proinflammatory genes. *Circulation.* 1999;100(12):1330–1337.
25. Satoh A, Shimosegawa T, Fujita M, et al. Inhibition of nuclear factor-kappaB activation improves the survival of rats with taurocholate pancreatitis. *Gut.* 1999;44(2):253–258.
26. Schreck R, Meier B, Mannel DN, Droge W, Baeuerle PA. Dithiocarbamates as potent inhibitors of nuclear factor kappa B activation in intact cells. *J Exp Med.* 1992;175(5):1181–1194.
27. Vega MI, Jazirehi AR, Huerta-Yepez S, Bonavida B. Rituximab-induced inhibition of YY1 and Bcl-xL expression in Ramos non-Hodgkin's lymphoma cell line via inhibition of NF-kappa B activity: role of YY1 and Bcl-xL in Fas resistance and chemoresistance, respectively. *J Immunol.* 2005;175(4):2174–2183.
28. Sheehan M, Wong HR, Hake PW, Malhotra V, O'Connor M, Zingarelli B. Parthenolide, an inhibitor of the nuclear factor-kappaB pathway, ameliorates cardiovascular derangement and outcome in endotoxic shock in rodents. *Mol Pharmacol.* 2002;61(5):953–963.
29. Perez DM, Papay RS, Shi T. alpha1-Adrenergic receptor stimulates interleukin-6 expression and secretion through both mRNA stability and transcriptional regulation: involvement of p38 mitogen-activated protein kinase and nuclear factor-kappaB. *Mol Pharmacol.* 2009;76(1):144–152.
30. Lv XB, Xie F, Hu K, et al. Damaged DNA-binding protein 1 (DDB1) interacts with Cdh1 and modulates the function of APC/CCdh1. *J Biol Chem.* 2010;285(24):18234–18240.
31. Liang Y, Zhong Z, Huang Y, et al. Stem-like cancer cells are inducible by increasing genomic instability in cancer cells. *J Biol Chem.* 2010;285(7):4931–4940.
32. Van Laere SJ, Van der Auwera I, Van den Eynden GG, et al. Nuclear factor-kappaB signature of inflammatory breast cancer by cDNA microarray validated by quantitative real-time reverse transcription-PCR, immunohistochemistry, and nuclear factor-kappaB DNA-binding. *Clin Cancer Res.* 2006;12(11, pt 1):3249–3256.
33. Van Laere SJ, Van der Auwera I, Van den Eynden GG, et al. NF-kappaB activation in inflammatory breast cancer is associated with oestrogen

receptor downregulation, secondary to EGFR and/or ErbB2 overexpression and MAPK hyperactivation. *Br J Cancer.* 2007;97(5):659–669.
34. Berlin O, Samid D, Donthineni-Rao R, Akeson W, Amiel D, Woods VL Jr. Development of a novel spontaneous metastasis model of human osteosarcoma transplanted orthotopically into bone of athymic mice. *Cancer Res.* 1993;53(20):4890–4895.
35. Fisher JL, Mackie PS, Howard ML, Zhou H, Choong PF. The expression of the urokinase plasminogen activator system in metastatic murine osteosarcoma: an in vivo mouse model. *Clin Cancer Res.* 2001;7(6): 1654–1660.
36. Cross DA, Alessi DR, Cohen P, Andjelkovich M, Hemmings BA. Inhibition of glycogen synthase kinase-3 by insulin mediated by protein kinase B. *Nature.* 1995;378(6559):785–789.
37. Jimi E, Aoki K, Saito H, et al. Selective inhibition of NF-kappa B blocks osteoclastogenesis and prevents inflammatory bone destruction in vivo. *Nat Med.* 2004;10(6):617–624.
38. Kishida Y, Yoshikawa H, Myoui A. Parthenolide, a natural inhibitor of nuclear Factor-kappaB, inhibits lung colonization of murine osteosarcoma cells. *Clin Cancer Res.* 2007;13(1):59–67.
39. Sourbier C, Danilin S, Lindner V, et al. Targeting the nuclear factor-kappaB rescue pathway has promising future in human renal cell carcinoma therapy. *Cancer Res.* 2007;67(24):11668–11676.
40. Enneking WF, Spanier SS, Goodman MA. A system for the surgical staging of musculoskeletal sarcoma. 1980. *Clin Orthop Relat Res.* 2003;(415): 4–18.
41. Hoeflich KP, Luo J, Rubie EA, Tsao MS, Jin O, Woodgett JR. Requirement for glycogen synthase kinase-3beta in cell survival and NF-kappaB activation. *Nature.* 2000;406(6791):86–90.
42. Wilson W III, Baldwin AS. Maintenance of constitutive IkappaB kinase activity by glycogen synthase kinase-3alpha/beta in pancreatic cancer. *Cancer Res.* 2008;68(19):8156–8163.
43. Eto M, Kouroedov A, Cosentino F, Luscher TF. Glycogen synthase kinase-3 mediates endothelial cell activation by tumor necrosis factor-alpha. *Circulation.* 2005;112(9):1316–1322.
44. Teo H, Ghosh S, Luesch H, et al. Telomere-independent Rap1 is an IKK adaptor and regulates NF-kappaB-dependent gene expression. *Nat Cell Biol.* 2010;12(8):758–767.
45. Villalobos V, Naik S, Bruinsma M, et al. Dual-color click beetle luciferase heteroprotein fragment complementation assays. *Chem Biol.* 2010;17(9): 1018–1029.

Funding

This work was supported by grants from the National Natural Science Foundation of China (30872967 to JW, 30973504 to J-NS, 30930045 and 81125015 to TK), from Guangdong NSFC (8251008901000019 to J-NS and 10251008901000000 to TK), from the Ph.D. program foundation of the Ministry of Education of China (20060558018 to J-NS and 20100171110079 to TK) and from the 973 project (2010CB912201 and 2012CB967000 to TK).

Notes

We thank Dr Jiong Deng (Shanghai Jiaotong University School of Medicine) for kindly providing the p65, luciferase reporter of p65 and the mutant form of IκBα (IκBα-mut) plasmids and the members of the laboratory for their helpful comments on the article. The funders had no roles in the design of this study, analysis or interpretation of the data, the writing of this article, and the decision to submit the article for publication.

Affiliations of authors: State Key Laboratory of Oncology in South China, Sun Yat-Sen University Cancer Center, Guangzhou, China (Q-LT, X-BX, QC, YL, Z-QZ, B-CY, R-HZ, Q-SF, W-GD, X-FZ, Y-XZ, TK); Department of Musculoskeletal Oncology (Q-LT, X-BX, JW, C-YZ, J-QY, Z-QZ, J-NS) and Department of Pathology (A-JH, D-WL), First Affiliated Hospital, Sun Yat-Sen University, Guangzhou, China; Department of Molecular and Cellular Biochemistry and Markey Cancer Center, University of Kentucky College of Medicine, Lexington, KY (BPZ).